Renormalization-group study of one-dimensional systems with roughening transitions

G. Bianconi,[1] M. A. Muñoz,[2,3] A. Gabrielli,[1,4,5] and L. Pietronero[1]
[1]*Dipartimento di Fisica and Unità di INFM, Università of Roma ''La Sapienza,'' I-00185 Roma, Italy*
[2]*The Abdus Salam International Centre for Theoretical Physics (ICTP), P.O. Box 586, 34100 Trieste, Italy*
[3]*Instituto de Física Teórica y Computacional, ''Carlos I.'', Facultad de Ciencias, Universidad de Granada, 18071 Granada, Spain*
[4]*Università di Roma ''Tor Vergata,'' I-00133 Roma, Italy*
[5]*Laboratoire de Physique de la Matière Condensée, Ecole Polytechnique, 91128 Palaiseau Cedex, Paris, France*
(Received 17 February 1999)

A recently introduced real-space renormalization-group technique, developed for the analysis of processes in the Kardar-Parisi-Zhang universality class, is generalized and tested by applying it to a different family of surface-growth processes. In particular, we consider a growth model exhibiting a rich phenomenology even in one dimension. It has four different phases and a directed percolation-related roughening transition. The renormalization method reproduces extremely well all of the phase diagram, the roughness exponents in all the phases, and the separatrix among them. This proves the versatility of the method and elucidates interesting physical mechanisms. [S1063-651X(99)05410-0]

PACS number(s): 05.40.−a, 05.20.−y, 05.70.Fh

I. INTRODUCTION

Surfaces and interfaces may grow in a smooth way or alternatively in a rough fashion. The study of the physical mechanisms originating these different behaviors has been the focus of an overwhelming number of recent studies [1–3]. The Kardar-Parisi-Zhang (KPZ) [4] equation is the minimal continuous model capturing the aforementioned physics. In dimensions larger than 2 it may exhibit two different phases: a flat and a rough one. Separating both of them there is a *roughening transition*. Apart of being a milestone in surface-growth theory, the KPZ equation is also related to other interesting physical problems: The Burgers equation in turbulence [5], directed polymers in random media [6], and systems with multiplicative noise [7], among others.

While the physics of the KPZ flat phase is very well understood, elucidating the properties of the rough phase has proven a puzzling problem [1,8,9]. In fact, standard field-theoretical analysis finds an unavoidable difficulty: The rough phase regime is controlled by a strong coupling fixed point, not accessible by standard perturbation techniques. Therefore, from a field-theory point of view not much can be concluded about the rough phase (recent interesting results in this direction can be found in [9–11]). An alternative strategy has been recently proposed to deal with this elusive problem; namely, a real-space renormalization-group (RSRG) approach. Its nonperturbative nature permits a direct access to the strong coupling regime and, in particular, gives estimations of the roughness exponent in dimensions ranging from $d=1$ to $d=9$ [12–14] (see also [15]) with results in very good agreement with the best numerical measurements [16]. Moreover, the same method has provided analytical evidence for the absence of an upper critical dimension for the KPZ strong-coupling phase [13], which has been a highly debated subject [17]. Additionally, it has also permitted us to analyze the behavior of the simpler linear surface-growth model, i.e., the Edwards-Wilkinson (EW) equation [14].

In this paper we intend to go further in the application and get an understanding of this RSRG approach. In particular, we study a class of systems exhibiting roughening transitions even in one dimension, by renormalizing them with the RSRG approach. Our motivation for that is twofold; on one hand we want to test the RSRG method (which was specifically devised to deal with KPZ growth) when generalized and apply it to other physical situations, i.e., we intend to analyze its versatility to deal with different physical problems. On the other hand, by doing so we will perform a renormalization of the class of systems exhibiting a roughening transition in $d=1$, that allows us to get some insight into their interesting physics.

The paper is structured as follows. In Sec. II we present a family of models exhibiting a one-dimensional roughening transition, and review their main properties. In Sec. III we present a generic two-parametric model in this class suitable to be renormalized using the RSRG approach, and discuss in detail all the different phases and physical behaviors. In Sec. IV we briefly present the main traits of the RSRG approach, discuss its application to our model, and present a detailed discussion of the results. In Sec. V the conclusions are presented.

II. SYSTEMS WITH ONE-DIMENSIONAL ROUGHENING TRANSITIONS

In this section we review the class of models exhibiting a one-dimensional roughening transition. The first studied model in this class is the so-called polynuclear growth model introduced by Kerstez and Wolf (KW) [18]. Its dynamics is defined by two successive steps: In the first one, particles are deposited (parallel) with probability p at each site of a one-dimensional lattice. In the second one, the terraces (kinks) formed by the previous deposition process grow laterally in a deterministic way by u units (or less if less space is available on the terrace). That is, kinks move deterministically increasing always the averaged height [18]. These two processes are iterated in time. For every u there is a critical value of p, p_c, such that for $p>p_c$ the surface grows homogeneously, is flat, and moves with maximal velocity [18]. The roughness expo-

nent in this flat regime is $\alpha=0$ and $\beta=0$ [19]. On the other hand, for $p<p_c$ steps are less likely to annihilate and the surface becomes rough. In this phase the roughness exponent is estimated to be $\alpha\approx 0.5$ and $\beta\approx 0.33$, compatible with their corresponding KPZ values. The roughening transition, as we discuss below, and as first pointed out by KW, is related to directed percolation (DP) [20].

After the seminal work by KW other models proposed for rather different physical problems have appeared in the literature, exhibiting similar phenomenology.

Alon *et al.* [21] proposed a model with absorption of particles and desorption at the edges of grown islands. This mimics the fact that in crystal growth particles absorbed in the interior of grown islands are more strongly bounded than particles on the edges. Their model is sequentially updated, and for large values of the absorbing probability the system is rough ($\alpha\approx 0.5$, and $\beta\approx 0.33$, compatible with their corresponding KPZ values), while for smaller values of the growing probability, the desorption mechanism has a larger relative importance, small islands are more easily eliminated, and the asymptotic behavior is flat ($\alpha\approx\beta\approx 0$). Moreover, these authors identify also a spontaneously broken symmetry in the model in the flat phase [21]. The phase transition in this case is also related to DP.

More recently an apparently unrelated model has been formulated in order to describe fungal growth; a fungal colony grows invading an environment, with the peculiarity that the local growth probability is non-Markovian [22]. With this main ingredient, and considering a triangular lattice, López and Jensen [22] found a roughening transition between a rough EW phase and a flat regime.

All the aforementioned models share a common property: The roughening transition can be related to a DP transition [20,23]. Having introduced this class of DP-related roughening transitions, in the next section we present a new model, in this same generic class, which turns out to be more suitable to be studied using the RSRG.

III. THE MODEL

Instead of trying to directly renormalize any of the previously defined models, we find it more convenient to define a model with the same generic phenomenology. The reason for this is that in the new model it seems that there is no proliferation of new relevant parameters when the proposed renormalization-group (RG) transformation is applied (for a more detailed discussion about proliferation of parameters in this scheme see [14]), and, therefore, the RG flow and the fixed point structure can be analyzed in a simple way. This does not exclude, in principle, the possibility of renormalizing directly any of the previously described models.

The model describes a surface driven by three different physical processes: deposition, evaporation, and condensation of particles on a one-dimensional lattice, $i=1,\ldots,L$ (generalizations to higher dimensions being straightforward). At each lattice site we associate an integer non-negative variable $h(i)$. The random deposition process corresponds to an external flux of particles, and occurs at each time step with probability p. The other two processes, i.e., evaporation and condensation, decrease the height difference between neighbor sites, and constitute therefore a smoothening source.

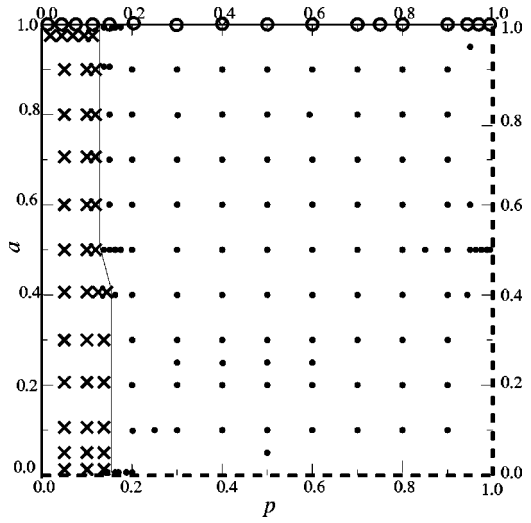

FIG. 1. System phase diagram. Filled circles (●) denote points in the Edward-Wilkinson universality class, crosses (×) denote points in the flat class, empty circles (○) denote points in the self-similar class, and dashed lines denote points in the random deposition class.

These occur with complementary probability $1-p$ at each time step, and they are responsible for the generation of correlations among different sites.

We consider flat initial configurations [$h(i)=0\ \forall i$ at $t=0$], periodic boundary conditions [24] [$h(1)=h(L)\ \forall t$], and sequential updating. The dynamics is defined by the following algorithm: At each simulation step a lattice site i_0 is selected randomly. Its height can either be increased by one unit with probability p (random deposition),

$$h(i_0)\rightarrow h(i_0)+1, \tag{1}$$

or alternatively, with complementary probability $1-p$; the surface is smoothened away (evaporation or condensation) in the following way:

$$h(i_0)\rightarrow h(i_0)+\mathrm{int}[a(h(i_0+1)-h(i_0))],$$

$$h(i_0)\rightarrow h(i_0)+\mathrm{int}[a(h(i_0-1)-h(i_0))], \tag{2}$$

where $a\in[0,1]$. Each one of these two possible events occurs with equal probability $(1-p)/2$. This process causes a decrease of the height difference (smoothening) between the site i_0 and one of its neighbors. In the dynamical rule given by Eq. (2) we have introduced the integer part function to enforce the height variables to take integer values.

Let us now discuss the model phenomenology. We have investigated the parameter space (p,a) with analytical and computational methods in different points as shown in Fig. 1. The evolution of the surface width can belong to one out of four different scaling regimes depending on the parameter values, p and a. These four universality classes define four qualitatively different growth morphologies, the corresponding typical surface profiles of which are shown in Fig. 2. They correspond to the following universality classes: The Edwards-Wilkinson [25,1–3], the *flat*, the *self-similar*, and the *random deposition* [1–3] universality class.

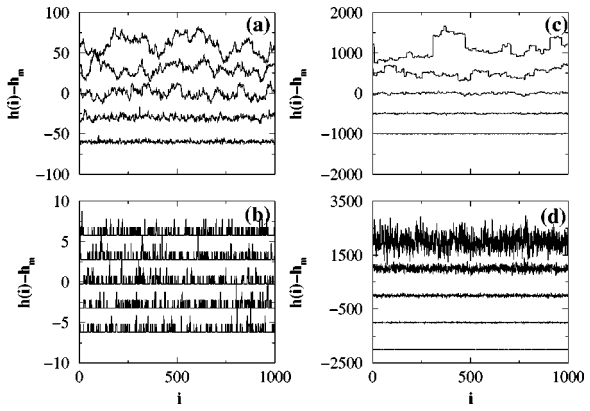

FIG. 2. Evolution profiles for the different universality class at times (from bottom to top) $t=10, 10^2, 10^3, 10^4$, and 10^5 for $L=1000$. (a) ($p=0.4$, $a=0.5$) corresponding to the Edwards-Wilkinson class, (b) ($p=0.1$, $a=0.5$) in the flat class, (c) ($p=0.75$, $a=1.0$) in the self-similar class, and (d) ($p=1$, $a=0.5$) in the random deposition class. Curves at $t=10^4$ and 10^5 ($t=10,10^2$) are shifted upward (downward) for the sake of clarity.

A. Edwards-Wilkinson universality class

The EW class is characterized by critical indexes $\alpha=1/2$, $\beta=1/4$, and $z=2$ [1–3]. We observe this type of scaling for parameter values $p>p_c(a)$, [where $p=p_c(a)$ is the separatrix between this phase and the flat one] with $p\neq 1$ and $a\neq 0,1$ (see Fig. 1 where points in this class are marked with filled circles). In Fig. 3(a) we show the collapse of the surface width for different system sizes (see figure caption). The best curve collapse is obtained for $\alpha=0.50\pm 0.01$ and $\beta=0.25\pm 0.01$ in agreement with the system being in the Edwards-Wilkinson universality class. This phase has a mean growing velocity different from zero (i.e., grows continuously in time) and has a rough surface appearance as shown in Fig. 2(a). In order to further confirm that the model is in the EW universality class and not in the KPZ one we have computed the dependence of the averaged velocity on the tilt [3], and verified that there is none, i.e., the velocity is a constant for every fixed tilt (at least for values of p sufficiently above the roughening transition, for which numerical accuracy is better).

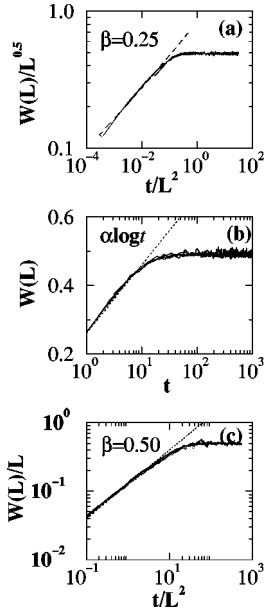

FIG. 3. Width evolution for system sizes $L=32$, 50, 64, 90, 128, and 256, for three different pairs of parameter values corresponding to (a) the Edwards-Wilkinson universality class, $(p,a)=(0.4,0.5)$; (b) the flat universality class, $(p,a)=(0.1,0.5)$; and (c) the self-similar universality class, $(p,a)=(0.75,1.0)$. In (a) and (c) the width is rescaled with L^{α} and plotted versus the time rescaled with L^z, with $\alpha=0.50\pm 0.01$, $\beta=0.25\pm 0.01$ in (a), and $\alpha=1.00\pm 0.02$, $\beta=0.50\pm 0.03$ in (c). In (b) a semilogarithmic scale is used; there is a logarithmic dependence on time for $t<10$, and a system size independent saturation width, compatible with $\alpha=0.00\pm 0.01$ and $\beta\sim 0$.

Let us present here a simple argument showing why this rough phase is EW-like and not KPZ-like. For that, we calculate the mean over different runs of the quantity $h(i,t+\Delta)$ (where $\Delta t=1/L$ is a time increment) for a fixed configuration $h(i,t)$ at time t. We can write

$$\langle h(i,t+\Delta t)\rangle - h(i,t)=\frac{p}{L}+\frac{1}{L}\frac{(1-p)}{2}a(h(i+1,t)-h(i,t)) \tag{3}$$

$$+\frac{1}{L}\frac{(1-p)}{2}a(h(i-1,t)-h(i,t)) \tag{4}$$

$$=\frac{p}{L}+\frac{(1-p)}{2L}a(h(i+1,t)+h(i-1,t)-2h(i,t)), \tag{5}$$

where it can be seen that there are two different contributions to the local velocity at each site i; the contribution coming from deposition, proportional to p, and the term arising from the smooth away processes. Observe that in this calculation we have neglected the effect of the integer part function, which we assume to be irrelevant in this phase (i.e., we expect it to reduce the mean velocity but not to change qualitatively the behavior [26]).

Dividing Eq. (5) by Δt and performing the thermodynamic limit, i.e., $L\to\infty$ (or equivalently $\Delta t\to 0$), we obtain

$$\left\langle \frac{\partial h(x)}{\partial t}\right\rangle = p+\frac{(1-p)}{2}a\nabla^2 h(x,t), \tag{6}$$

which corresponds to differential evolution of the Edwards-Wilkinson equation (averaged over noise) driven by an external constant force p. The main point of this calculation is that it shows that the dynamics is controlled by a Laplacian term, and no gradient square terms appear. Therefore, the model is expected to be in the EW universality and not in the KPZ one. For $p=1$ or $a=0$ this equation describes random deposition as, in fact, is the case in our model. Equation (6) fails to describe the growth of our model in the cases $p\leqslant p_c$ or $a=1$. In fact, as stated before, in Eq. (5) the integer part function has been neglected and this approximation is incorrect when (i) $p\leqslant p_c$, the fluctuations of the surface are small, and the rounding-off mechanism due to the integer part function takes over, pinning and flattening the surface, and (ii) in the case $a=1$, for which in the absence of smooth-

ening, the continuum limit has to be taken more carefully. In this last case, we expect the dynamics to be controlled by the diffusion of height steps.

B. Flat universality class

This universality class is characterized by critical indexes $\alpha=0$ and $\beta=0$ (with logarithmic corrections). We observe this phase for parameter values: $p<p_c(a)$ with $p\neq 0$ and $a\neq 0,1$. In Fig. 1 we plot points in this class with crosses in the parameter space. In this phase, height fluctuations are independent on sample size (i.e., $\alpha=0$), the mean surface velocity is zero in the thermodynamic limit, and the lowest level ($h=0$) is occupied with a finite density as shown in Fig. 2(b). Due to finite-size effects, finite systems in this class may have a nonvanishing velocity.

In Fig. 3(b) we have plotted in a semilogarithmic scale the surface width versus time for different system sizes (see figure caption). Observe that the width has a logarithmic dependence on t for short times,

$$W(t)\propto \log(t). \tag{7}$$

For all the different points in this phase, by employing data-collapse techniques we evaluate $\alpha=0.00\pm 0.05$ and $\beta=0$ with logarithmic corrections.

The existence of this phase is due to the fact that for small values of p the deposition process is more unlikely than the smoothening one, and there is a physical constraint preventing the surface to go below the lowest, $h=0$ level. The integer part function in the dynamic rules favors the evaporation process by giving an extra negative drift term with respect to Eq. (6). This extra term binds the surface to the lowest level making it flat for small values of p. In particular, for a fixed value of a, the roughening transition corresponds to the value of p for which this extra negative term is equal to $-p$. For values of p slightly larger than that critical value the surface unbinds and grows with constant velocity.

C. Self-similar universality class

This class is characterized by $\alpha=1$, $\beta=1/2$, and $z=2$; it is observed for parameter values $a=1$ and $p\neq 0,1$, which are plotted in Fig. 1 with empty circles. In Fig. 3(a) we show the collapse of the width for different system sizes (see figure caption); from the best data collapse we measure $\alpha=1.00\pm 0.02$ and $\beta=0.50\pm 0.03$. The surface in this regime is, therefore, self-similar; that is, height fluctuations are of the order of magnitude of the system size [see also Fig. 2(c) where a typical profile is shown]. In this case, contrary to $a\neq 1$ we observe no roughening transition (except for a trivial one at $p=0$.)

Observe that for $a=1$ the dynamical rules can be written as

$$\begin{aligned} h(i_0,t)&=h(i_0,t-1)+1 \quad \text{with Prob } p,\\ h(i_0,t)&=h(i_0+1,t-1) \quad \text{with Prob } (1-p)/2,\\ h(i_0,t)&=h(i_0-1,t-1) \quad \text{with Prob } (1-p)/2, \end{aligned} \tag{8}$$

where the integer part function, being redundant, has been omitted. Therefore, the extra negative driving term, arising as a consequence of the integer part function in the dynamics (which, as discussed in the previous subsection, favors evaporation) does not exist in this case. This explains why there is no roughening transition for $a=1$.

The main qualitative physical difference between this phase, the EW, and the flat phases, is that here there is no smoothening of height gradients. Large steps diffuse in space due to the effect of the second and third rules in Eq. (8), but do not smooth away, creating a much rougher surface.

Now we study the mean-field solution of this case, obtained by neglecting spatial correlations. This turns out to be an useful calculation as we will show afterwards.

The master equation for the probability $P(h,t)$ for a given site to have a height value h at time t is

$$\begin{aligned} \frac{\partial P(h,t)}{\partial t}&=pP(h-1,t)-pP(h,t)+(1-p)P(h,t)\\ &\quad -(1-p)P(h,t)\\ &=p[P(h-1,t)-P(h,t)], \end{aligned} \tag{9}$$

where we have assumed nearest-neighbor sites to have the same probability distribution as the site under consideration. Equation (9) is the same equation that we would obtain if we considered a mean-field approximation of the random deposition process. In order to solve Eq. (9), it is convenient to introduce the generating function defined as

$$G(x,t)=\sum_{h=0}^{\infty} x^h P(h,t), \tag{10}$$

with the normalization condition $G(1,t)=1\ \forall\, t$. The master equation written in terms of $G(x,t)$ reads

$$\frac{\partial G(x)}{\partial t}=p[xG(x,t)-G(x,t)]=p(x-1)G(x,t). \tag{11}$$

By taking derivatives with respect to the dummy variable x, one can write

$$\begin{aligned} W^2(t)=\langle h^2-\langle h\rangle^2\rangle&=[\partial_x^2 G(x)+\partial_x G(x)]\big|_{x=1}\\ &\quad -[\partial_x G(x)|_{x=1}]^2. \end{aligned} \tag{12}$$

Taking time derivatives of both sides and integrating the resulting equation, we finally obtain $W(t)=\sqrt{pt}$, and, consequently, $\beta=1/2$. On the other hand, the height differences among neighbors (or steps) perform a random diffusion in the direction perpendicular to the growth. Like in the case of a random walker the average step displacement scales as the square root of time. But the effective time for step displacement is $(1-p)t$, and, therefore, in order to cover a distance L, a characteristic time

$$t\sim L^2/(1-p) \tag{13}$$

is needed. Consequently, the dynamical exponent is $z=2$. Combining this result with the fact that $\beta=1/2$, we obtain $\alpha=1$ just by using the scaling relation $\alpha=z/\beta$. Therefore, the values of the critical exponents found in mean-field approximation agree perfectly with the numerical results. Moreover, the mean-field approximation also reproduces the

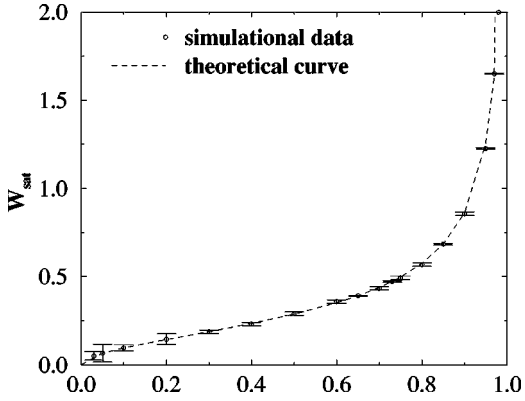

FIG. 4. Saturated width of a system of size $L=64$ with $a=0.5$, as a function of p. The data are extremely well fitted by the mean-field prediction.

dependence of the saturation width as a function of p for a fixed system size. In fact, using $W(t)=\sqrt{pt}$ and Eq. (13) we find

$$W_{sat}(p)\sim L\sqrt{\frac{p}{(1-p)}} \tag{14}$$

in perfect agreement with the simulation results as shown in Fig. 4.

D. Random deposition universality class

The random deposition class is characterized by $\alpha=\infty$ and $\beta=1/2$. With dashed lines in Fig. 1 we have plotted the two lines in this class, namely, those given by the conditions $a=0$ and $p=1$, respectively. For these values the only physical mechanism present is the random deposition of particles. In this phase the surface is spatially uncorrelated, and its roughness increases rapidly with time, with $\beta=1/2$, and there is no width saturation ($z=\infty$) as shown in Fig. 2(d).

E. The roughening transition

As stated previously, both in our model and in the previously discussed ones, the transition between the flat and the rough phase belongs to the percolation DP universality class. The reason for this can be explained by mapping the dynamics in a directed percolationlike model. In order to do this in our model (for the others, similar mappings can be performed), we introduce a new set of variables $\{s_i\}$ defined as

$$\begin{aligned} s_i&=1 \quad \text{if} \quad h(i)=0, \\ s_i&=0 \quad \text{if} \quad h(i)\neq 0. \end{aligned} \tag{15}$$

By studying the evolution of these variables we focus our attention on the lowest height level occupation. This information is enough to describe the phase transition [18] as we show in what follows. A site i with $s_i=1$ corresponds to an occupied (active) site in a DP-like model (or better, in a contact process model, which is a sequentially updated version of DP [20]). On the contrary, $s_i=0$ for empty (absorbing) sites of the DP-like model. The deposition process may change with probability p an occupied, $s_i=1$, site into an unoccupied, $s_i=0$, site. This same mechanism is also present in the contact process [20]. On the other hand, the smoothening mechanism, occurring with probability $1-p$, may induce [27] the ''infection'' of an empty site by a neighboring active site as in the contact process. In this language, the flat surface phase corresponds to the DP active phase, and the rough phase corresponds to the absorbing one. The key feature is that in absorbing regions (that is, in regions with $s_i=0$), activity cannot be generated spontaneously. This is the main physics of DP and, therefore, the critical behavior at the roughening transition is related to the transition into an absorbing phase of DP and related models.

By using this mapping the scaling of some magnitudes can be related to DP exponents. In particular, the density of sites at the lowest level n_0 should scale as a function of the distance to the critical point, $\varepsilon=|p-p_c|$, like $n_0\sim\varepsilon^{\beta_{DP}}$. Right at the critical point n_0 decays in time as $n_0(t)\sim t^{-\theta_{DP}}$. For finite systems of size L,

$$n_0\sim L^{-\beta_{DP}/\nu_{\perp,DP}}\sim L^{-x_f}, \tag{16}$$

where $\nu_{\perp,DP}$ is the correlation length exponent. Finally, the mean surface velocity is inversely proportional to the life time $\tau=|\varepsilon|^{-\nu_{\parallel,DP}}$ of the DP active phase, where $\nu_{\parallel,DP}$ is the usual correlation time exponent. Therefore,

$$v\sim\varepsilon^{-\nu_\parallel}\sim L^{-\nu_\parallel/\nu_\perp}\sim L^{-x_v}. \tag{17}$$

The one-dimensional DP values of the previously introduced exponents are $\beta_{DP}=0.27649(4)$, $\theta=0.15947(3)$, $x_f=0.25208(5)$, and $x_v=1.58074(4)$ (numbers in parentheses denote uncertainties in the last figure) [28].

In order to verify numerically if the previous prediction holds we have studied extensively the $a=0.5$ case. We have performed numerical simulations in order to determine critical exponents, to be compared with their corresponding DP values. In particular, by considering a system size $L=3000$, and averaging over 8000 independent runs, we measure n_0 as a function of time. A power-law decay is observed at (the critical point) $p_c=0.13740\pm0.00005$, with an associated exponent

$$\theta=0.160\pm0.003, \tag{18}$$

in good agreement with its DP value. Using the previously estimated value of the critical point, we measure the stationary density of sites at the lowest layer $h=0$ for $p<p_c$. In Fig. 5(b) we show the data for $\varepsilon\in[10^{-4},10^{-1}]$. Performing a fit for small values of ε we find

$$\beta_{DP}=0.275\pm0.007, \tag{19}$$

also in good agreement with its DP value. By performing a finite-size scaling analysis, we determine $x_f=0.250\pm0.03$ and $x_v=1.57\pm0.01$ to be compared with their corresponding DP values $x_f=0.25208(3)$ and $x_v=1.5807(5)$, respectively. Numerical data are shown in Figs. 5(c) and 5(d).

Summing up, all the measured exponents confirm the hypothesis that the roughening transition is controlled by a DP fixed point.

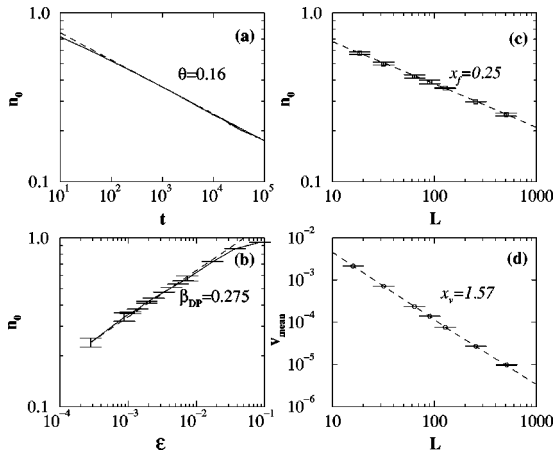

FIG. 5. Critical indexes characterizing the DP transition. (a) Log-log plot of the density of sites at the lowest level as a function of time at (0.1374,0.5); the associated critical exponent is $\theta = 0.160 \pm 0.003$. (b) Log-log plot of the asymptotic density of states at the lowest site versus $\varepsilon = p_c - p$; from the slope we measure $\beta_{DP} = 0.275 \pm 0.007$. In (c) and (d) we report the density of sites at the lowest level and the mean velocity at the critical point for different system sizes. The corresponding critical indexes are $x_f = 0.250 \pm 0.003$ and $x_v = 1.57 \pm 0.01$.

IV. RENORMALIZATION APPROACH

Having described in detail the model phenomenology, in this section we apply the RSRG technique recently proposed [12–14] to renormalize our model. For a detailed description of the method we refer the reader to Ref. [14]. In a nutshell the RG method consists of two main ingredients. One is the definition of cells of generic substrate length $L_k = 2^k L_0$ (where L_0 is the length of the minimal relevant substrate scale) and height h_k, with which the space in which the surface grows can be covered; cells are progressively invaded by the growing surface (see Fig. 6). The second one is

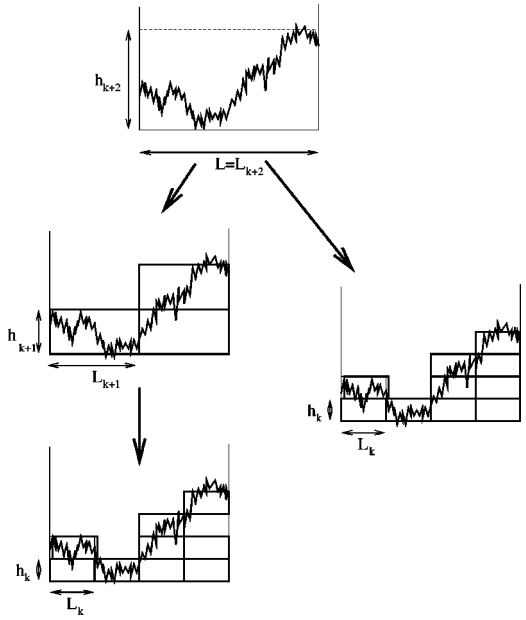

FIG. 6. A system of size $L_{k+2} = 4L_k$ can be studied composed of four cells of size L_k, or alternatively by iterating twice a partition in cells of half length. See text.

the identification of the effective dynamics of these cells at a generic scale; that is, one studies the effective rules by which cells are progressively invaded by the growing surface at a given scale. This effective dynamics is described by parameters that change upon changing the scale of description. In our case we have a set of parameters $\mathbf{x}_k = (a_k, p_k)$ at scale L_k. Knowing the effective dynamics at scale L_k, defined by $\mathbf{x}_k$ and the associated width at that scale W_k, the renormalization problem consists of determining what the width values are of W_{k+m} and the effective dynamic parameters $\mathbf{x}_{k+m}$ at a coarser scale L_{k+m}. This problem was analyzed in [12–14], with the final conclusion that one can write,

$$W_{k+m}^2 = W_k^2 F_m(\mathbf{x}_k), \tag{20}$$

where $F_m(\mathbf{x}_k) = 1 + 4w^2(m, \mathbf{x}_k)$ and $w(m, \mathbf{x}_k)$ is the width of a system composed of 2^m cells of unitary height with a dynamics driven by the parameters $\mathbf{x}_k$. These last functions can be determined by means of a rather inexpensive Monte Carlo simulation. The width at scale $k+2$ can be calculated in two different ways: (i) by direct use of the previous formula with $m = 2$, or alternatively, (ii) by iterating twice the previous transformation with $m = 1$. Imposing that both the previous procedures give the same result for the width W_{k+2}, one obtains a renormalization condition, namely, [12,14]

$$x_{k+1} = F_1^{-1}(F_2(x_k)/F_1(x_k)). \tag{21}$$

For monoparametric models this equation is enough to determine the evolution under RG transformations of the effective parameter x_k, and from it all the scale-invariant physics can be elucidated [12–14]. In the present two-parametric dynamics it is necessary to consider another independent analogous equation, corresponding to calculating the width at scale $k+3$ in two different ways,

$$\begin{aligned} \mathbf{x}_{k+1} &= F_1^{-1}(F_2(\mathbf{x}_k)/F_1(\mathbf{x}_k)), \\ \mathbf{x}_{k+1} &= F_2^{-1}(F_3(\mathbf{x}_k)/F_1(\mathbf{x}_k)). \end{aligned} \tag{22}$$

The first equation is just Eq. (21), and the second states that the width obtained by dividing the system in eight cells should be the same as the width obtained dividing first the system in two blocks, and then each of these blocks in four subcells. This set of equations give the (discrete) flux of the effective dynamics parameters upon coarse graining. The scale-invariant dynamics is determined by the fixed point (or points) of Eq. (22), $\mathbf{x}^*$ for which

$$\begin{aligned} F_1(\mathbf{x}^*) &= F_2(\mathbf{x}^*)/F_1(\mathbf{x}^*), \\ F_2(\mathbf{x}^*) &= F_3(\mathbf{x}^*)/F_1(\mathbf{x}^*), \end{aligned} \tag{23}$$

is satisfied. Once $\mathbf{x}^*$ is known, the α exponent is easily determined by

$$\alpha = \tfrac{1}{2}\log_2[F_1(\mathbf{x}^*)]. \tag{24}$$

In order to evaluate the F_1, F_2, and F_3 functions we have performed Monte Carlo simulations for a system of size $L = 2,4,8$, and averaged, once the stationary state is reached for long enough times. We have determined these functions

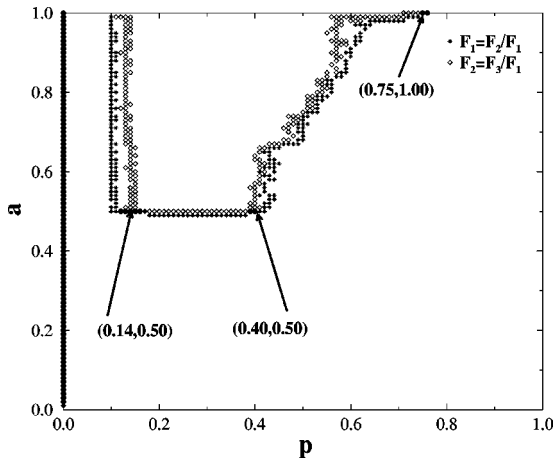

FIG. 7. The two lines (marked, respectively, with diamonds and empty circles) correspond to the values for which $F_1(\mathbf{x}) = F_2(\mathbf{x})/F_1(\mathbf{x})$ and $F_2(\mathbf{x}) = F_3(\mathbf{x})/F_1(\mathbf{x})$, within the numerical error, respectively. The intersection points of these two lines define the dynamic fixed points, invariant under RG flow. See text.

on the sites of a 100×100 lattice in the parameter space, that is, for values of p and a multiples of 0.01.

In Fig. 7 we show the curves corresponding to $F_1 = F_2/F_1$ and $F_2 = F_3/F_1$. The intersecting points of these curves are the RG fixed points within numerical accuracy. We find the following stable fixed points:

$$p=0.75,\ a=1,\ \text{corresponding to}\ \alpha=1.00\pm0.02,$$

$$p=0.40,\ a=0.5,\ \text{corresponding to}\ \alpha=0.50\pm0.01, \tag{25}$$

$$p=0,\ \forall\, a,\ \text{corresponding to}\ \alpha=0.00\pm0.01,$$

while at $(p,a)=(0.14,0.5)$ there is an unstable fixed point. The stability is determined by observing whether nearby points flow into the fixed point or flow away from it, under application of Eq. (22), and the corresponding values of α are determined using Eq. (24).

We have also determined different renormalization flux lines as shown in Fig. 8. Observe that each continuous flow line in Fig. 8 has been constructed by joining together consecutive points obtained from renormalization-group equations (22) (which determine a discrete iterative mapping and not a continuous flow). Observe that the lines defined by $a = 0.5$ and $a=1$ define invariant manifolds.

The accordance between the renormalization flow diagram (Fig. 8) and the phase diagram independently found with simulation on large systems (Fig. 1) is very good (compare Figs. 1 and 8). In particular, (a) For all points yielding in the EW phase we find trajectories converging to the stable fixed point (0.4,0.5) with $\alpha=0.5\pm0.01$, in perfect agreement with the EW value. (b) The separatrix in Fig. 1 is reproduced quite accurately in Fig. 8; in particular, the unstable fixed point (0.14,0.5) is located on it. (c) Points to the left of the separatrix (i.e., points in the flat phase) flow towards the fixed line at $p=0$ for which $\alpha=0$ (corresponding to the flat phase). (d) All points with $a=1$ and $p>0$, i.e., in the self-similar phase, flow to a fixed point at (0.75,1) with $\alpha=1.00\pm0.01$.

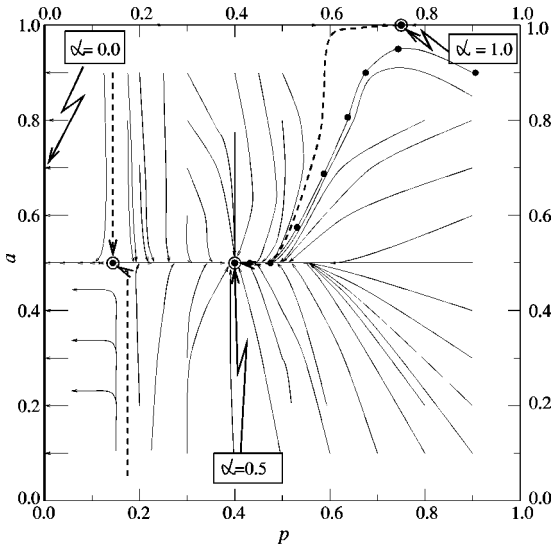

FIG. 8. Renormalization-group flow for Eq. (2). The stable fixed points are $p=0.4$, $a=0.5$ (EW behavior); $p=0.75$, $a=1$ (self-similar phase); p, $\forall\, a$ (flat phase); and the unstable point $p=0.14$, $a=0.5$ (corresponding to a DP transition). For the flux line starting at (0.95,0.95), we show explicitly the points found by iterating the renormalization-group equations. To guide the eye discrete sequences of points obtained by iteration of the RG transformation are plotted as continuous lines.

We have verified all the above conclusions to be stable when more refined RSRG algorithms are considered. That is, instead of considering bypartitions and quadripartitions of a given growing surface, one can consider larger partitions, and the technique described above remains the same in spirit [12,14]. By doing this, we observe all the above-described results to remain unaltered. This stability, upon changes in the RSRG details, supports the fact that no new relevant parameters have to be introduced upon renormalization to describe the scale-invariant dynamics [14], i.e., the scale-invariant dynamics is well described at an arbitrary scale by the found fixed points.

V. CONCLUSIONS

We have discussed different growth models exhibiting a one-dimensional roughening transition. In particular, we have introduced a two-parametric model capturing the main physics of this type of roughening transition, i.e., exhibiting a rough and a flat phase, and a critical line separating them, related to directed percolation. The model has the technical advantage that no new parameter proliferate upon renormalization. Apart from the previously discussed phenomenology, the model exhibits also a self-similar phase. All the different phases and transitions have been analyzed by means of extensive numerical simulations and some analytical approaches.

We have renormalized this model by using a recently introduced RSRG approach. In particular, fixed points, corresponding to the scale-invariant dynamics are found, and the

corresponding roughness exponent determined. The results are in perfect accordance with all the numerical and analytical findings. In particular, the phase diagram is perfectly reproduced: The rough, flat, and self-similar phases, as well as the separatrix among them and their associated roughness exponents, are identified with great accuracy.

This confirms the general validity of the RSRG method to deal with anisotropic fractal growth in cases others than KPZ growth for which it was explicitly designed.

ACKNOWLEDGMENTS

We acknowledge interesting discussions with M. Marsili, G. Parisi, Y. Tu, and W. Genovese. We especially thank C. Castellano for very useful comments, suggestions, and a critical reading of the manuscript. This work has been partially supported by the European Network under Contract No. FMRXCT980183, and by the Spanish Ministerio de Educación under Project Nos. DGESIC and PB97-0842.

[1] T. Halpin-Healy and Y.-C. Zhang, Phys. Rep. **254**, 215 (1995).

[2] J. Krug and H. Spohn, in *Solids Far From Equilibrium*, edited by C. Godreche (Cambridge University Press, Cambridge, 1990); J. Krug, Adv. Phys. **46**, 139 (1997).

[3] A.L. Barabási and H.E. Stanley, *Fractal Concepts in Surface Growth* (Cambridge University Press, Cambridge, 1995).

[4] M. Kardar, G. Parisi, and Y.C. Zhang, Phys. Rev. Lett. **56**, 889 (1986).

[5] See D. Forster, D.R. Nelson, and M.J. Stephen, Phys. Rev. A **16**, 732 (1977), and references therein.

[6] D.A. Huse, C.L. Henley, and D.S. Fisher, Phys. Rev. Lett. **55**, 2924 (1985). See also [1] and [2].

[7] G. Grinstein, M.A. Muñoz, and Y. Tu, Phys. Rev. Lett. **76**, 4376 (1996); Y. Tu, G. Grinstein, and M.A. Muñoz, *ibid.* **78**, 274 (1997).

[8] E. Medina, T. Hwa, and M. Kardar, Phys. Rev. A **39**, 3053 (1989); M. Lässig Nucl. Phys. B **448**, 559 (1995).

[9] M. Lässig, J. Phys.: Condens. Matter **10**, 9905 (1998).

[10] E. Frey, U.C. Taüber, and H.K. Janssen, Europhys. Lett. **47**, 14 (1999); Eur. Phys. J. B **9**, 491 (1999).

[11] M. Marsili and A.J. Bray, Phys. Rev. Lett. **76**, 2750 (1996).

[12] C. Castellano, M. Marsili, and L. Pietronero, Phys. Rev. Lett. **80**, 4830 (1998).

[13] C. Castellano, A. Gabrielli, M. Marsili, M.A. Muñoz, and L. Pietronero, Phys. Rev. E **58**, R5209 (1998).

[14] C. Castellano, M. Marsili, M.A. Muñoz, and L. Pietronero, Phys. Rev. E **59**, 6460 (1999).

[15] M. A. Muñoz, G. Bianconi, C. Castellano, A. Gabrielli, M. Marsili, and L. Pietronero, Comput. Phys. Commun. (to be published).

[16] T. Ala-Nissila *et al.*, J. Stat. Phys. **72**, 207 (1993); L.-H. Tang *et al.*, Phys. Rev. A **45**, 7162 (1992). See also [17].

[17] M. Lässig and H. Kinzelbach, Phys. Rev. Lett. **78**, 903 (1997); T. Ala-Nissila, *ibid.* **80**, 887 (1998); J.M. Kim, *ibid.* **80**, 888 (1998); M. Lässig and H. Kinzelbach, *ibid.* **80**, 889 (1998).

[18] J. Kertész and D.E. Wolf, Phys. Rev. Lett. **62**, 2571 (1989).

[19] The usual scaling ansatz for the width W is $W(L,t)=\langle(h-\langle h\rangle)^2\rangle^{1/2}$ in a substrate of length L at time t is $W(L,t)=L^{\alpha}f(t/L^{z})$ with $f(x)\sim x^{\beta}$ for $x\ll 1$, and $f(x)\sim$const for $x\gg 1$. The critical indices α, β, and z are connected by $z=\alpha/\beta$ [see F. Family and T. Vicsek, J. Phys. A **18**, L75 (1985)].

[20] J. Marro and R. Dickman, *Nonequilibrium Phase Transitions* (Cambridge University Press, Cambridge, 1998); G. Grinstein and M. A. Muñoz, in *Fourth Granada Lectures in Computational Physics*, edited by P. Garrido and J. Marro (Springer, Berlin, 1997); in *Springer Lecture Notes in Physics* Vol. 493, edited by P. Garrido and J. Marro (Springer, Berlin, 1997), p. 223, and references therein.

[21] U. Alon, M.R. Evans, H. Hinrichsen, and D. Mukamel, Phys. Rev. Lett. **76**, 2746 (1996); Phys. Rev. E **57**, 4997 (1998).

[22] J.M. López and H.J. Jensen, Phys. Rev. Lett. **81**, 1734 (1998).

[23] One-dimensional roughening transitions related to classes of systems with absorbing states; others than directed percolation can also be found. See S. Park and B. Khang, e-print cond-mat/9807193 (unpublished); H. Hinrichsen and G. Odor, Phys. Rev. Lett. **82**, 1205 (1999), and references therein. See also P. Bhattacharyya, Int. J. Mod. Phys. (to be published).

[24] We have verified that all our conclusions remain unchanged when open; instead of periodic, boundary conditions are considered.

[25] S.F. Edwards and D.R. Wilkinson, Proc. R. Soc. London, Ser. A **381**, 17 (1982).

[26] In fact, the mean velocity from slightly above the critical point p_c to $p=1$ can be calculated by subtracting to p the averaged loss due to the effect of the integer part function. Assuming that a is a rational number that can be written as $a=m/n$ and supposing that all height differences among nearest neighbors are equally probable, one readily obtains that the velocity can be written as $v=p-(1-p)m(n-1)/(2n)$. This result fits extremely well the numerical results in the noncritical region (i.e., above $p=0.25$ the fit is perfect).

[27] Observe that in the case $a=1$, given the absence of the integer part function, this infection mechanism is not present.

[28] M.A. Muñoz, R. Dickman, A. Vespignani, and S. Zapperi, Phys. Rev. E **59**, 6175 (1999).